

Isotope-shift measurement of the NO_2^- gap mode spectrum in KI with persistent ir spectral holes

W. P. Ambrose and A. J. Sievers

Laboratory of Atomic and Solid State Physics and Materials Science Center,
Cornell University, Ithaca, New York 14853-2501

(Received 4 August 1988)

Persistent infrared spectral holes are used to identify the isotope shifts of the far-infrared gap modes associated with NO_2^- in KI. Two of the modes are determined to be translational while the third has a mixed translational-librational character. The properties of the mixed mode disagree in a fundamental way with the predictions of the previous lattice-dynamical calculation for this defect-lattice system.

The vibrational properties of NO_2^- in KI have long attracted interest because of the apparent conflicting signature of this substitutional defect when measured with different spectroscopic probes. One striking property is the orthogonality between direct far-infrared absorption (FIR) and the Raman scattering results produced by this C_{2v} defect for impurity modes in the gap between the acoustic and optic-phonon branches of the host crystal.^{1,2} To account for this puzzling result Evans and Fitchen¹ noted that since parity appears to be a good quantum number the C_{2v} defect must not distort the cubic symmetry of the I^- cavity. On the other hand, parity is not conserved in the model of Rebane, Zavt, and Haller² where the detailed lattice-dynamical calculations of Zavt³ are used to characterize the translational and librational motion of the molecule in the lattice. Their fit has been made with anisotropic force constants at the defect site so that the threefold degenerate translational mode associated with an isotropic defect is split. Two translational gap modes bracket a third mode which has a mixed translational and librational character. In their model, it is this librational character which causes the different spectroscopic results since it makes the intermediate mode strongly Raman active and only weakly FIR active.²

The discovery that tunable ir diode lasers can burn persistent ir spectral holes (PIRSH's) in vibrational modes gives a new method for analyzing this system.⁴ The technique consists of PIRSH burning in the internal ir mode spectrum of NO_2^- in KI and simultaneously measuring the FIR changes with interferometry. Our first measurements showed that three FIR gap modes with comparable strengths occur for NO_2^- in KI, not two as previously determined, and that the Raman-active mode is still not coincident with any of these transitions.⁵ Since three FIR- and Raman-active gap modes are allowed for a C_{2v} molecule, the origin of the entire FIR spectrum is once again open to question. The possibility that this spectrum is mainly translational^{6,7} or librational⁸ in character or even that the Raman and FIR results obey the parity selection rule just as for a point defect¹ in a cubic lattice is still unresolved.

In this paper we make the first identification of the isotope effect on the FIR gap-mode spectrum by PIRSH burning and establish it as the technique *par excellence*

for assigning spectral lines to a particular isotopic species of NO_2^- . The substitution of ^{18}O for ^{16}O and ^{15}N for ^{14}N in NO_2^- produces gap-mode frequency shifts for two of the three modes consistent with translational mode behavior. The ^{15}N for ^{14}N substitution also demonstrates that the intermediate mode for the most abundant isotopic species does have some librational character even though it does not appear in the Raman spectrum. This new level of FIR sensitivity confirms that the two spectroscopic techniques do probe orthogonal aspects of the defect dynamics.

Since isotopically enriched NO_2^- is not readily available, NO_3^- enriched with either 40% ^{18}O or 99% ^{15}N has been used as the dopant. The crystals are grown by the Czochralski method under an atmosphere of Ar so that roughly 99% of the NO_3^- decomposes into NO_2^- . For the KI boules which contain nearly pure (14,16,16) and (15,16,16) NO_2^- species, the concentration is determined from the peak absorption coefficient in the ir stretch region at room temperature.⁸ However, the complexity of the stretch-mode spectrum in the mixed ^{16}O - ^{18}O dopant crystals, which contain the same order of magnitude of (14,18,18), (14,16,18), and (14,16,16), requires a different technique to determine concentrations.

At 1.5 K the infrared-absorption strength of the $(\nu_2 + \nu_3)$ vibrational combination mode is comparable in strength to the FIR gap modes. The relation between the molecule concentration N and the combination line peak absorption coefficient α_c or integrated line strength S_c is

$$N = [(3.6 \pm 0.2) \times 10^{17} \text{ ions/cm}^2] \alpha_c, \quad (1)$$

$$= [(8 \pm 1) \times 10^{18} \text{ ions/cm}] S_c,$$

where $S_c = \int \alpha dv$. Table I identifies the vibrational-combination-mode frequency $(\nu_2 + \nu_3)$ for the isotopes.

The main spectroscopic tools for the PIRSH measurements consist of a high-resolution (0.03 cm^{-1}) Fourier-transform infrared (FTIR) instrument in combination with a tunable ir diode laser.⁵ PIRSH's are burned into the internal vibrational-mode spectrum of NO_2^- at 1.5 K to reveal gap-mode changes belonging to the reoriented defect. For example, by burning on the sharp internal-bending mode of a single NO_2^- isotopic species (the ν_2

TABLE I. Some infrared vibrational-mode frequencies of isotopic NO_2^- in KI.

Isotopic species	ν_2 (cm^{-1})	$\nu_2 + \nu_3$ (cm^{-1})
14,16,16	804.85	2044.89
15,16,16	799.93	...
14,16,18	785.90	2009.90
14,18,18	766.65	1981.12

frequency is given in Table I), all FIR gap modes induced by the isotope are distinguished. The hole may be erased by warming the crystal above 8 K. At that temperature the rapidly reorienting molecules redistribute themselves among the 12 possible orientations, one of which is illustrated in Fig. 1. It should be noted that this hole burning is not a simple consequence of the off-center behavior of NO_2^- in KI since PIRSH burning also is found for the KBr and KCl hosts where the molecule is known to be on center.⁹

Figure 2 shows the impurity induced spectrum obtained for a KI crystal doped with 0.1 mol% KNO_3 with 40% ^{18}O enrichment. The lines near 73, 78, and 87 cm^{-1} appear to be isotopically shifted NO_3^- modes. The broad features at 92 and 94 cm^{-1} do not show an oxygen-isotope shift and their source is unknown. PIRSH burning on the ν_2 bending mode of the (14,16,18) species with laser polarization parallel and perpendicular to the interferometer beam axis produces the FIR spectral changes shown in Figs. 2(b) and 2(c). Traces Figs. 2(d) and 2(e) show the gap-mode changes produced by burning the (14,18,18) ir bending mode with the same two laser polarizations. Our investigation indicates that only spectral lines within those grouped near 71 and 79 cm^{-1} in Fig. 2 are induced by the different isotopes of the NO_2^- molecule. Without the PIRSH labeling technique, unambiguous mode identification would be difficult in this mixed mode spectrum.

Table II contains the spectral information obtained for these isotopically shifted modes. The center frequency ν , the full width at half maximum Γ , and the line strength S/N where $S = \int \alpha(\nu) d\nu$ of each line are presented. The sum of the line strengths $\Sigma(S/N)$, shown in the last column, is found (within experimental error) to be in-

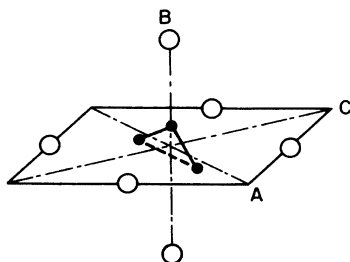


FIG. 1. One orientation of the NO_2^- molecule in the octahedral site. During PIRSH burning the anisotropic molecule reorients among the 12 equivalent arrangements in the KI host. The principle axes of the molecule are labeled A, B, and C.

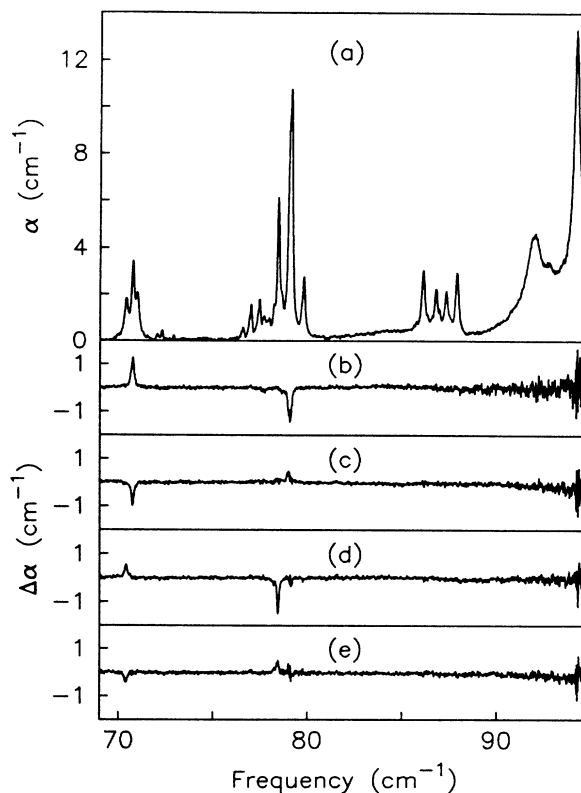


FIG. 2. The effect of hole burning the isotope shifted ir bending mode of NO_2^- on the FIR gap modes in KI. (a) The spectrum for KI nominally doped with 0.1% KNO_3 (40% ^{18}O enrichment). (b) and (c) are the FIR gap-mode absorption changes produced by burning the (14,16,18) ir ν_2 mode with laser polarization parallel and perpendicular to the interferometer beam axis. (d) and (e) are the gap-mode changes produced by burning the (14,18,18) ir ν_2 mode with laser polarization parallel and perpendicular to the interferometer beam axis.

dependent of the particular isotopic species. This result demonstrates that the induced spectral components remain in the gap region for all isotopic combinations in accord with the principle of spectroscopic stability.¹⁰

The systematic frequency shifts associated with the individual spectral components can be seen most easily when presented as line strengths versus frequency for the different species as shown in Fig. 3. The bar heights give the line strengths for a particular species. In the (14,16,16) or the (15,16,16) single-species spectra, each strong mode has a corresponding weak mode to its low-frequency side consistent with a gap-mode shift due to the natural abundance of host crystal K^+ isotopes.⁵ For the mixed-isotope crystal with (14,18,18), (14,18,16), and (14,16,16) species, the close grouping of the lines precludes an identification of any weak modes so accurate Lorentzian fits have been obtained using the strong modes shown in Fig. 2; however, it should be recognized that an equal number of weak modes may also be present in these spectra.

The vertical location of each spectrum in Fig. 3 is positioned so that the expected isotope shift for a translational mode should be described by a straight line (dashed line in

TABLE II. KI:NO₂⁻ isotopically shifted gap-mode spectral information.

Isotopic species	ν (cm ⁻¹)	Γ (FWHM) (cm ⁻¹)	S/N (10 ⁻¹⁹ cm)
14,16,16	70.463	0.197	0.36 ± 0.01
	70.985	0.197	4.24 ± 0.19
	79.000	0.132	1.07 ± 0.03
	79.124	0.135	5.80 ± 0.20
	79.698	0.117	1.07 ± 0.03
	79.804	0.122	3.57 ± 0.13
			$\Sigma(S/N) = 16.1 \pm 0.6$
15,16,16	70.340	0.220	0.50 ± 0.05
	70.828	0.186	4.17 ± 0.33
	78.145	0.157	1.28 ± 0.10
	78.417	0.130	5.83 ± 0.36
	79.397	0.150	1.14 ± 0.09
	79.510	0.131	3.85 ± 0.23
			$\Sigma(S/N) = 16.8 \pm 1.1$
14,16,18	70.730	0.163	3.49 ± 0.33
	78.616	0.196	1.18 ± 0.12
	79.015	0.124	3.19 ± 0.30
	79.112	0.175	6.68 ± 0.61
			$\Sigma(S/N) = 14.5 \pm 1.4$
14,18,18	70.386	0.180	3.58 ± 0.33
	78.204	0.123	1.29 ± 0.12
	78.438	0.128	9.11 ± 0.66
			$\Sigma(S/N) = 14.0 \pm 1.1$

Fig. 3). The translational gap-mode frequency can be parametrized by

$$\omega_0^2 = \frac{K}{M + M^*}, \quad (2)$$

where K is the effective spring constant of the mode, M is the molecule mass, and M^* is the contribution to the normal mode from the lattice. For the small-isotope effect the frequency shift $\Delta\omega$ is proportional to the mass change ΔM measured from the abundant (14,16,16) species labeled by (M_0, ω_0) where

$$\Delta\omega = - \left[\frac{\omega_0}{2(M_0 + M^*)} \right] \Delta M. \quad (3)$$

The linear dependence shown by Eq. (3) is represented by the nearly vertical dashed lines in Fig. 3 which connect the frequencies of one species to the next. The lowest- and highest-frequency spectral lines follow the linear ΔM behavior expected for translational modes but the intermediate frequency mode for the abundant species does not. This mode is not pure librational in character since no systematic dependence is found in the observed frequency shift versus the moment of inertia about any of the three molecular axes; however, the unusual mass dependence

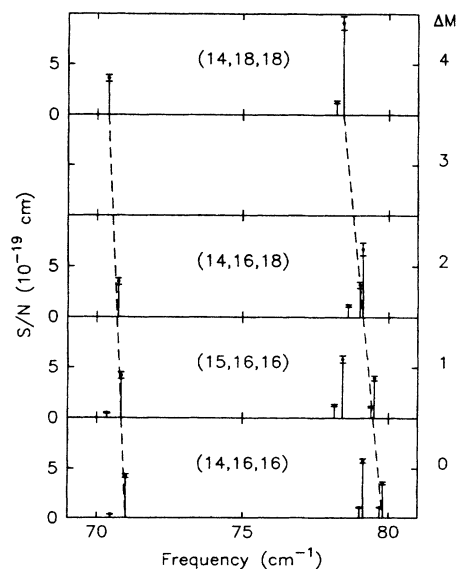


FIG. 3. Gap-mode line strengths of the different NO₂⁻ isotopic species vs frequency. The isotopic mass of the molecule is identified in the figure by (N, O, O) . Note the sum of the line strengths is the same for each species. The right ordinate gives ΔM the isotopic mass change and the dashed line the isotope shift expected for translational mode behavior.

shown in Fig. 3 indicates that some librational contribution about the A axis, as defined in Fig. 1, must occur.

The high-resolution identification of only one mixed translational-librational and two translational modes completely characterizes the ir active gap-mode spectrum of the NO_2^- molecule in KI. Since a single line is observed between 75 and 76 cm^{-1} in Raman scattering,^{1,2} no overlap exists between the FIR and the Raman results. The original explanation of this difference requires that parity be a good quantum number so that the two kinds of spectroscopies give mutually exclusive results.¹ In this picture the Raman-active mode is identified with an E_g symmetry gap mode vibration. Rebane *et al.*² have shown that such a low-frequency E_g mode would require the corresponding ir active T_{1u} mode to be unstable. On the other hand, their model specifies that one of the three gap modes, in fact the ir active translational-librational mode with libration about the A axis, occurs at the Raman frequency. This coincidence is not observed in our measurements. In order to miss detecting a fourth ir active mode, it would have to be 200 times weaker than the three modes we have observed.

Neither explanation can account for both types of data and still be consistent with theory; however, perhaps the parity conservation proposal can be combined with the idea of anharmonic local modes. A new concept¹¹ is that crystalline anharmonicity makes allowed localized as well as plane-wave phonon modes in pure crystals at finite temperatures and that in impure crystals these anharmonic localized modes can be trapped at defect centers at low temperatures. Within this framework the harmonic E_g mode could occur at a much larger frequency (say, 133 cm^{-1} by Ref. 1) than the T_{1u} mode consistent with the mode stability requirement and the unexpected Raman-active E_g gap mode (and even lower-frequency T_{2g} mode) would result from anharmonic modes weakly bound to the defect site.

This research has been supported by the U.S. Army Research Office (USARO) Grants No. DAAG29-85-0206 and No. DAAL03-86-K-0103 and by the National Science Foundation Grant No. DMR-85-16616 through the Materials Science Center at Cornell University.

¹A. R. Evans and D. B. Fitchen, *Phys. Rev. B* **2**, 1074 (1970).

²L. A. Reband, G. S. Zavt, and K. E. Haller, *Phys. Status Solidi (b)* **81**, 57 (1977).

³G. S. Zavt, *Phys. Status Solidi (b)* **80**, 399 (1977).

⁴A. J. Sievers and W. E. Moerner, in *Persistent Spectral Hole-Burning: Science and Applications*, edited by W. E. Moerner (Springer-Verlag, New York, 1988), Chap. 6.

⁵W. P. Ambrose and A. J. Sievers, *Chem. Phys. Lett.* **147**, 608 (1988).

⁶A. J. Sievers and C. D. Lytle, *Phys. Lett.* **14**, 271 (1965).

⁷K. F. Renk, *Phys. Lett.* **14**, 281 (1965).

⁸V. Narayanamurthi, W. D. Seward, and R. O. Pohl, *Phys. Rev.* **148**, 481 (1966).

⁹H. S. Sack and C. M. Moriarty, *Solid State Commun.* **3**, 93 (1965).

¹⁰C. H. Townes and A. L. Schawlow, *Microwave Spectroscopy* (McGraw-Hill, New York, 1955), p. 344.

¹¹A. J. Sievers and S. Takeno, *Phys. Rev. Lett.* **61**, 970 (1988).